Observation of an Energy- and Temperature-Dependent Carrier Mass for Mixed-Valence CePd₃

B. C. Webb[a] and A. J. Sievers

Laboratory of Atomic and Solid State Physics and Materials Science Center, Cornell University, Ithaca, New York 14853

and

T. Mihalisin

Department of Physics, Temple University, Philadelphia, Pennsylvania 19122
(Received 9 December 1985)

The far-infrared conductivity of CePd₃ has been obtained from temperature-dependent reflectivity measurements between 0.4 and 400 meV. The low-temperature results are consistent with simple Fermi-liquid ideas, even though the conduction-carrier density is less than 0.3 electron per formula unit.

The mixed-valence compound CePd₃ has been under theoretical[1,2] and experimental investigation[2] in recent years because it represents a class of systems in which dramatic low-temperature transport properties are thought to be produced by the interaction between the conduction electrons and the partially filled $4f$ level of the rare-earth ion. Implicit in the interpretation of the very large thermopower,[3] Hall constant,[4] and specific-heat[5] coefficients has been the assumption that the carrier density is on the order of three to four electrons per formula unit. The electronic structure within a few millielectronvolts of the Fermi energy has already been probed by infrared measurements, but all of these studies have failed to make a connection between the dc and the ir results. Room-temperature ir measurements,[6] which cover many decades in frequency, show normal-metal behavior, while low-temperature measurements,[7] which do show anomalous absorptivity, have been made over too restricted an interval to provide a direct measure of the carrier density.

In this Letter we report on temperature-dependent reflectivity measurements between 0.4 and 400 meV for CePd₃ and identify both bound- and free-carrier contributions to the low-temperature conductivity. A temperature-independent carrier density whose value corresponds to less than 0.3 electron per formula unit is the source of the low-frequency conduction. The far-infrared conductivity can be explained by Fermi-liquid theory with a "free"-carrier mass that is both frequency and temperature dependent.

The polycrystalline samples are prepared from stoichiometric amounts of the constituents by arc melting in an argon atmosphere and formed into 0.5-cm-diam disks using a mousetrap mold. These disks form one wall of a nonresonant cavity for the lowest-frequency absorptivity measurement. At higher frequencies (~ 12 meV) the sample absorptivity is so large that the cavity technique breaks down.[8] In this region a direct measurement of the reflectivity is made with two reflections at 45° angle of incidence but with a wave-guided beam. A lamellar or Michelson interferometer has been used in conjunction with a ³He-cooled bolometer detector to make these measurements. Above 120 meV the reflectivity is measured using strictly a ray-optics configuration. As an independent check, the reflectivity values at two fixed frequencies have also been obtained using laser sources (29.5 and 115 meV). Measurements have been extended at 300 K from 0.5 up to 5 eV using a CARY spectrometer and a near-normal–incidence three-bounce configuration.

Figure 1 shows the normal-incidence absorptivity for CePd₃ for three different temperatures. The solid line represents the data at 4.2 K, the dashed line at 77 K, and the dot-dashed line at 295 K. The two dashed vertical lines define the frequency interval over which temperature-dependent measurements have been made. Below 1 meV, the measured absorptivities are in close agreement with the classical skin-effect result calculated with the measured dc resistivities. With increasing frequency the 4.2-K data exhibit a 15-fold increase in absorptivity between 8 and 40 meV which persists at least to the notch near 300 meV. Over this entire region the enhanced absorptivity weakens with increasing temperature.

To obtain the optical parameters $\epsilon_1(\omega)$ and $\sigma_1(\omega)$, where

$$\tilde{\epsilon}(\omega) = \epsilon_1(\omega) + i(4\pi/\omega)\sigma_1(\omega), \qquad (1)$$

the absorptivity data are first extrapolated to $\omega = 0$ with the Hagen-Rubens relation; next the data at 300 K are used to extend the low-temperature data from 0.5 to 5 eV. Since the absorptivity retains some temperature
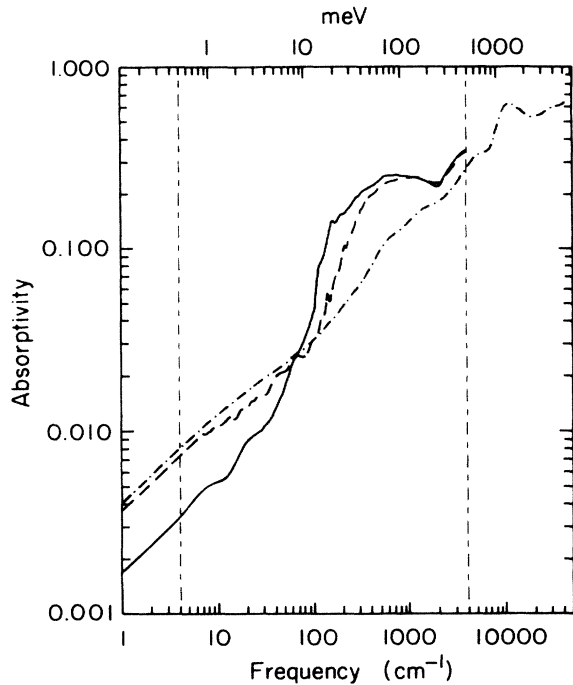
FIG. 1. Normal-incidence absorptivity of CePd$_3$ vs frequency. The different curves identify different temperatures: 4 K (solid), 75 K (dashed), and 295 K (dot-dashed). The vertical dashed lines identify the frequency interval over which temperature-dependent measurements have been made. The curves are extended below 0.5 meV with the classical skin-effect value determined from the measured dc resistivity. Room-temperature measurements were made from 5 meV to 5 eV. The instrumental resolution is typically 6% of the frequency.

FIG. 2. $\sigma_1(\omega)$ and $\epsilon_1(\omega)$ for CePd$_3$. The curves identify different temperatures: 4 K (solid), 75 K (dashed), and 295 K (dot-dashed). The zero-frequency limit of $\sigma_1(0)$ is set equal to the measured dc conductivity. At 4.2 K $\sigma_1(0)$ = 60×10^{15} s^{-1}.

dependence at 0.5 eV, it is necessary to join the two reflectivity curves in this region. We find that as long as the joint is smooth the low-frequency optical parameters are not significantly affected by the details of this connection. Finally, beyond our largest measured frequency the absorptivity is extrapolated to $\omega \rightarrow \infty$ with an ω^{-4} approximation. A Kramers-Kronig analysis[9] of the extended absorptivity curve gives the optical parameters $\epsilon_1(\omega)$ and $\sigma_1(\omega)$ shown in Fig. 2.

There is some value in attempting first a standard decomposition of Fig. 2. The room-temperature data (295 K) represented by the dot-dashed lines display the frequency dependences characteristic of a metal. In the infrared $\epsilon_1(\omega) < 0$, and the conductivity peaks in $\sigma_1(\omega)$ identify bound carriers, while at lower frequencies $\sigma_1(\omega)$ shows the characteristic Drude dependence for free carriers with a rolloff at about 30 meV. At 4.2 K the contributions from the free and bound electrons display prominent features in separate frequency regions. The lowest-frequency interband is located at 0.235 eV and the free-carrier conductivity is characterized by an extremely sharp spike centered at
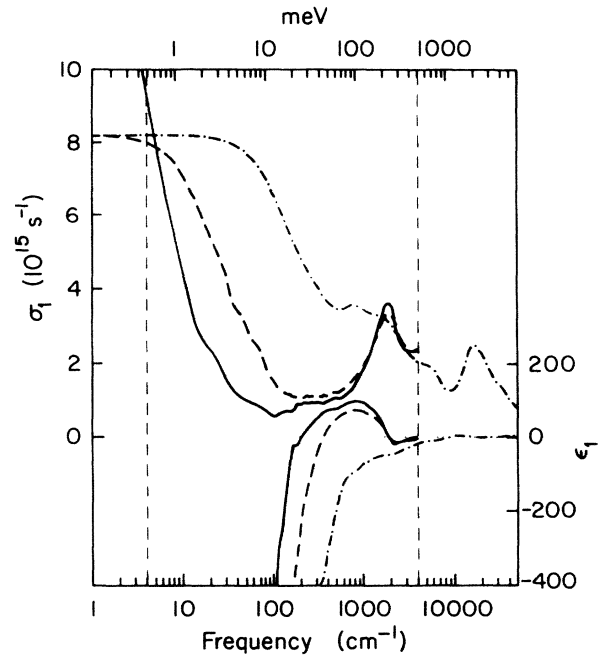
zero frequency. The dielectric response function is separated into contributions from free $[\sigma^f(\omega)]$ and bound $[\sigma^b(\omega)]$ carriers:

$$\sigma_1(\omega) = \sigma_1^f(\omega) + \sigma_1^b(\omega) \tag{2}$$

and

$$\epsilon_1(\omega) = (-4\pi/\omega)\sigma_1^f(\omega) + \epsilon_1^b(\omega) + \epsilon_\infty^b, \tag{3}$$

where in the far infrared, the Drude model is used to describe the free carriers; a Lorentz oscillator, the interband transition at 0.235 eV; and the constant screening term ϵ_∞^b, the higher-energy interbands. With this model a good fit can be obtained to the room-temperature data shown in Fig. 2. The free-carrier plasma frequency is obtained from the Drude contribution to $\sigma_1(\omega)$. We find $\omega_p^2 = 4\pi \times 10^{30}$ sec^{-2}.

Fits to the temperature-dependent data show that ϵ_∞^b is constant and that the 0.235-eV transition can be accurately described with a Lorentz oscillator of constant strength and position but temperature-dependent width. The surprising result is that although the low-temperature Drude parameters are energy independent for energies larger than 40 meV, for smaller values they are no longer constant.

Attempts to reproduce both the real and imaginary parts of the low-frequency dielectric function by adding another set of free or bound carriers to the
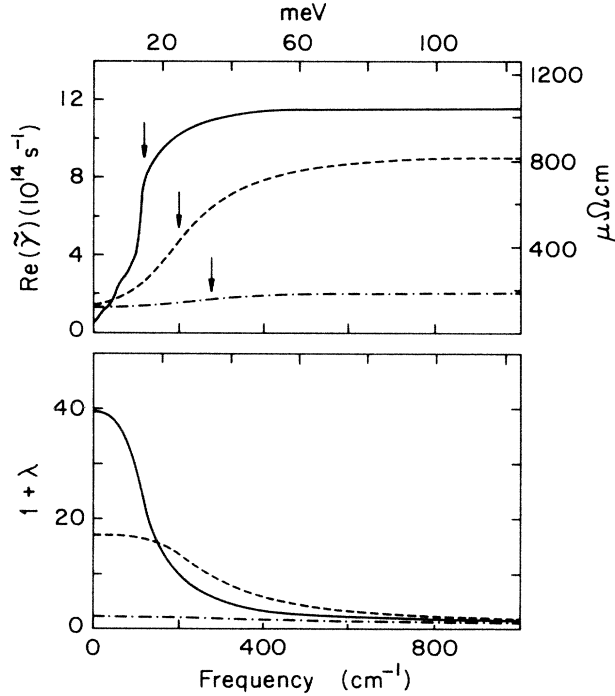
FIG. 3. Frequency-dependent parameters for the free carriers in CePd$_3$ at different temperatures. Top: frequency-dependent rate, Re[$\tilde{\gamma}(\omega)$]. Bottom: enhancement factor, $1+\lambda(\omega)$. Solid curves, 4.2 K; dashed curves, 75 K; and dot-dashed curves, 295 K. The magnitude of the frequency dependence decreases and the frequency position of the knee (arrow) increases with increasing temperature.

room-temperature model have failed; however, a physical picture consistent with the temperature- and frequency-dependent data is obtained when the Drude model is generalized to allow the free carriers to undergo frequency-dependent scattering while at the same time keeping this carrier density fixed at the room-temperature value.[10] The free-carrier conductivity equation now becomes

$$\tilde{\sigma}^f(\omega) = (\omega_p^2/4\pi)[\tilde{\gamma}(\omega) - i\omega]^{-1}, \qquad (4)$$

where the real and imaginary parts of $\tilde{\gamma}(\omega)$ are constrained by a Kramers-Kronig relation and $\omega_p^2 = 4\pi ne^2/m_b$, where m_b is the optical band mass. In the limit of zero frequency, Re$\tilde{\gamma}(\omega)$ approaches the dc scattering rate and Im$\tilde{\gamma}(\omega)$ tends to zero.

The top of Fig. 3 shows the frequency dependence of Re[$\tilde{\gamma}(\omega)$] as a function of temperature. At 4.2 K the scattering rate grows as ω^2 from a small value at zero frequency and then levels off at a constant value. This plateau may result from saturation of the scattering since the mean free path calculated from Re[$\tilde{\gamma}(\infty)$] and ω_p^2 is about one lattice constant. With increasing temperature, the shape of the frequency-dependent scattering rate does not change, although

the magnitude weakens and the knee moves to somewhat higher frequencies.

The consequences of frequency-dependent scattering have been derived for the electron-phonon interaction.[11,12] However, the analysis should be valid for frequency-dependent scattering arising from coupling of a Fermi liquid to any bosonic energy spectrum,[11] so that some of these ideas which have general applicability are outlined below. Associated with an interaction which produces a frequency-dependent scattering is the concomitant frequency-dependent renormalization of the quasiparticle effective mass. To display this dependence the conductivity [Eq. (4)] is rewritten in terms of a frequency-dependent scattering time and plasma frequency[12,13]:

$$1/\tau(\omega) = \text{Re}[\tilde{\gamma}(\omega)]/[1+\lambda(\omega)] \qquad (5)$$

and

$$\omega_p^2(\omega) = \omega_p^2/[1+\lambda(\omega)], \qquad (6)$$

where $\lambda(\omega) = -\text{Im}[\tilde{\gamma}(\omega)]/\omega$ and $1+\lambda(\omega)$ is the enhancement factor.

The traces at the bottom of Fig. 3 show the experimentally determined enhancement factor as a function of frequency and temperature. If $1+\lambda(\omega)$ is associated with the quasiparticle effective mass then the data can be interpreted as evidence that the carriers interact strongly at low temperature with a second low-frequency excitation spectrum which itself is not infrared active. At energies large compared to 20 meV, the electrons are no longer screened by the interaction and the effective mass reduces to the frequency-independent optical band mass m_b. At low frequencies, corresponding to long time scales and low energies, the mixed-valence $4f$ polarization strongly enhances the effective mass. The mass in this low-frequency limit is

$$m(0) = (1+\lambda_0)m_b, \qquad (7)$$

where $\lambda_0 = \lim_{\omega\to 0}\lambda(\omega)$. Figure 3 shows that at 4.2 K $\lambda_0 \approx 40$; hence the coupling is at least an order of magnitude larger than that observed for the electron-phonon interaction.[12] The coupling strength is directly related to the area under a mass-enhancement curve, since

$$\text{Re}[\tilde{\gamma}(\infty)] - \text{Re}[\tilde{\gamma}(0)] = \frac{2}{\pi}\int_0^\infty \lambda(\omega)\,d\omega. \qquad (8)$$

The temperature-dependent data in Fig. 3 show that this strength is a monotonic function of temperature and that almost no coupling remains by room temperature.

With the low-temperature mass-enhancement factor determined, it is now possible to obtain an estimate of the carrier density. In the Fermi-liquid picture the carriers which contribute at low temperatures to the spe-

cific heat should also be the carriers that contribute to the far-infrared conductivity. The coefficient for the linear term in the specific heat γ varies as[14]

$$\gamma \propto m_t n^{1/3}, \tag{9}$$

where m_t is the thermal mass. To relate the thermal mass m_t to the far-infrared mass $m(0)$ we assume that normal-metal arguments will prevail.[15] For a Fermi surface that does not intersect the Brillouin-zone boundary it can be shown that $m_t > m(0)$. In principle this relation can be reversed for an intersecting Fermi surface; however, it has been found empirically that the above inequality remains true in that case as well.

For the low-frequency, low-temperature limit we set

$$m_t \approx m(0) = (1 + \lambda_0) m_b;$$

then the combination of the specific heat[5] γ with our free-carrier plasma-frequency result, namely $\omega_p^2 = 4\pi \times 10^{30}$ sec^{-2}, gives the optical band mass, $m_b = 1 m_e$. It appears that the conduction-electron mass enhancement deduced from the frequency-dependent scattering rate is large enough to account for all of the free-carrier specific-heat enhancement. Note that the upper bound on the carrier density, $n = 4 \times 10^{21}$ cm^{-3}, is less than 0.3 carrier per formula unit.

From temperature-dependent reflectivity measurements covering three decades in frequency, both free- and bound-carrier contributions to the ir conductivity have been identified. Data analysis which includes frequency-dependent scattering of the free carriers shows that both the frequency and temperature dependences can be characterized with a small set of parameters. Although the metallic carrier density is surprisingly small, simple Fermi-liquid theory is consistent with this analysis. These carriers appear to be strongly coupled at low temperature to a second excitation spectrum which extends throughout the far infrared up to 15 meV; however, because the coupling is a strong function of temperature almost no trace of this unusual process remains at room temperature.

Note added.—Recently Varma[16] has pointed out that the exchange of spin fluctuations by conduction electrons would give rise to renormalizations in the electronic properties reminiscent of those produced by the electron-phonon interaction.

(a)Present address: Physics Department, University of California at San Diego, La Jolla, CA 92093.

[1]P. Coleman, P. W. Anderson, and T. V. Ramakrishnan, Phys. Rev. Lett. 55, 414 (1985).

[2]See, for example, Valence Instabilities, edited by P. Wachter and H. Boppart (North-Holland, Amsterdam, 1982).

[3]H. Sthioul, D. Jaccard, and J. Sierro, in Ref. 2.

[4]E. Cattaneo, U. Hafner, and D. Wohlleben, in Ref. 2.

[5]T. Mihalisin, P. Scoborea, and J. A. Ward, Phys. Rev. Lett. 46, 862 (1981).

[6]B. Hillebrandes, G. Guntherodt, R. Pott, W. König, and A. Breitschwerdt, Solid State Commun. 43, 891 (1982); J. W. Allen, R. J. Nemanich, and S.-J. Oh, J. Appl. Phys. 53, 2145 (1982); J. Schoenes and K. Andres, Solid State Commun. 42, 359 (1982).

[7]F. E. Pinkerton, B. C. Webb, A. J. Sievers, J. W. Wilkins, and L. J. Sham. Phys. Rev. B 30, 3068 (1984).

[8]B. C. Webb, A. J. Sievers, and T. Mihalisin, J. Appl. Phys. 57, 3134 (1985).

[9]J. S. Toll, Phys. Rev. 104, 1760 (1965).

[10]Although a two-band model or a frequency-dependent relaxation-time model may be adjusted to fit one part of the complex conductivity in the far infrared, each will produce its own unique signature in the other part. For an example of this point, see the discussion centered around Fig. 2 in A. J. Sievers, Phys. Rev. B 22, 1600 (1980).

[11]A. B. Pippard, in Optical Properties and Electronic Structure of Metals and Alloys, edited by F. Abelès (North-Holland, Amsterdam, 1966), p. 623; A. J. Leggett, Ann. Phys. (N.Y.) 46, 76 (1968).

[12]P. B. Allen, Phys. Rev. B 3, 305 (1971).

[13]J. W. Allen and J. C. Mikkelsen, Phys. Rev. B 15, 2952 (1977).

[14]P. Nozieres, Theory of Interacting Fermi Systems (Benjamin, Reading, MA, 1964), p. 7.

[15]F. Abelès, in Optical Properties of Solids, edited by F. Abelès (North-Holland, Amsterdam, 1972), p. 106.

[16]C. Varma, Phys. Rev. Lett. 55, 2723 (1985).